

## Metal Adsorption and Adhesion Energies on MgO(100)

Charles T. Campbell\* and David E. Starr

*Contribution from the Department of Chemistry, Box 351700, University of Washington, Seattle, Washington 98195-1700*

Received January 28, 2002

**Abstract:** The calorimetrically measured heats of adsorption of Cu, Ag, and Pb on MgO(100), previously measured in our group, are correlated with bulk properties of the metals and their sticking probabilities and film morphologies. The low-coverage heats of adsorption (when the metals are mainly in two-dimensional (2D) islands) are used to estimate metal–MgO(100) bond energies within a pairwise bond additivity model. These values correlate well with the observed initial sticking probabilities and saturation island densities of the metals. This supports a transient mobile precursor model for adsorption. The values also correlate with their bulk sublimation energies, which suggests that covalent metal–Mg bonding dominates the interaction at low coverage, probably due to very strong bonding at defects. The heats of adsorption integrated up to multilayer coverages provide the metal–MgO(100) adhesion energies and metal–MgO(100) bond energies for metals in 3D films. These values correlate with the sum of magnitudes of the metal's bulk sublimation energy plus the heat of formation of the bulk oxide of the metal per mole of metal atoms. This suggests that local chemical bonds, both metal–oxygen and covalent metal–Mg, dominate the interfacial bonding for 3D films.

### I. Introduction

The metal/oxide interface plays a key role in many technologically important applications, including novel structural materials based on metal/ceramic composites, metal/oxide seals in device and medical implant construction, metal/oxide contacts in microelectronics and photovoltaic devices, coatings for corrosion passivation, gas-sensors, and oxide-supported transition-metal catalysts. In the last example alone, it is obvious that the cost of a precious metal catalyst will be less if the catalyst can be spread across the surface of an inexpensive oxide support with a high fraction of the metal atoms actually on the surface (i.e., with high dispersion). Additionally, energy and operational costs can be reduced in this way. For this reason, industrial metal catalysts almost always utilize some oxide support material. The choice of support material and the method of its preparation is often dictated by the degree of spreading (dispersion) achieved by the active metal when placed on that support, but there is little fundamental understanding of relationships between dispersion and the oxide's surface structure and composition. However, it is clear that the bonding strength at the interface between the metal and the oxide must dictate the metal particles' morphology and sintering kinetics. The activity per unit metal area of a catalyst and its selectivity in many cases also depends directly on the size of the metal nanoparticles. Thus, learning to control dispersion can lead to more energetically efficient and environmentally friendly operation of these catalysts. In many other areas, economic and environmental issues are similarly influenced by successful control of the metal/oxide interface.

Until the past decade, little was known about the atomic-level structure at metal/oxide interfaces, about the electronic character of the metal atoms that are right at these interfaces, or about the thermodynamic stability of these interfaces. These are critical issues, since they must be intimately connected to technologically relevant parameters such as the hardness of composite materials, the peel strength of metal/oxide contacts, the efficiency of photovoltaic devices, the speed and size of microelectronics, the corrosion resistance of passivation layers, the sensitivity and lifetime of sensors, and the catalytic activity and selectivity of oxide-supported metal particles or cations.

A great deal of work in this area by a variety of investigators has recently improved our understanding of the metal/oxide interface considerably. The vapor deposition of metal films onto well-defined oxide surfaces under the clean conditions of ultrahigh vacuum has provided a controlled method for studying fundamental details concerning metal/oxide interfaces and metal particles or films on oxide surfaces. In this approach, all the tools of the surface scientists' trade can be brought to bear for structural and electronic characterization and for chemisorption studies with simple probe molecules. A number of very important reviews have recently appeared which discuss various aspects of this approach and the new insights it has provided.<sup>1–11</sup> It is now possible, for example, to prepare metal particles on

- (1) Bäumer, M.; Freund, H.-J. *Prog. Surf. Sci.* **1999**, *61*, 127.
- (2) Freund, H. J.; Bäumer, M.; Kühlenbeck, H. *Adv. Catal.* **2000**, *45*, 333.
- (3) Henry, C. R.; Chapon, C.; Giorgio, S.; Goyhenex, C. In *Chemisorption and Reactivity on Supported Clusters and Thin Films*; Lambert, R. M., Pacchioni, G., Eds.; Kluwer: Amsterdam, 1997; p 117.
- (4) Henry, C. R. *Surf. Sci. Rep.* **1998**, *31*, 231.
- (5) Campbell, C. T. *Surf. Sci. Rep.* **1997**, *227*, 1.
- (6) Gunter, P. L. J.; Niemantsverdriet, J. W. *Catal. Rev. Sci. Eng.* **1997**, *39*(1 and 2), 77.
- (7) Freund, H.-J. *Angew. Chem., Int. Ed. Engl.* **1997**, *36*, 452.

\* To whom correspondence should be addressed. E-mail: campbell@chem.washington.edu.

relatively defect-free single-crystalline oxide surfaces, where both the particles' thickness and lateral dimension (i.e. parallel to the surface) are known and controllable with nearly atomic accuracy. Also, these studies have revealed how the extreme proximity of an oxide's interface influences the chemisorptive or catalytic properties of a metal's surface when the metal films or particles are only one or two atomic layers thick.

However, little is known about the energetics of such metal particles. Yet energy is the dominant contributor to the thermodynamic driving force for any surface reaction steps involving these metal particles, such as metal-atom migration during metal particle sintering, particle redispersion or chemisorption, and reactions of gases on the particles. Furthermore, the equilibrium wetting and shape of the metal particles are determined by the adhesion energy of the metal/oxide interface, through Young's equation.<sup>12</sup> While temperature-programmed desorption (TPD) has been used to measure desorption energies (and thus adsorption energies) for a few metal-on-oxide systems,<sup>5,9,13–15</sup> late transition-metal particles rapidly sinter into large, poorly dispersed particles at much lower temperature than those required for metal-atom desorption. Thus, the desorption energies obtained by TPD are not for metal atoms in highly dispersed metal particles, which are of the greatest interest and which reveal the greatest insight into the strength of the metal–oxide bond.

Our group recently developed the unique ability to measure calorimetrically metal-atom adsorption energies at room temperature and below, where high dispersions can be obtained.<sup>16–22</sup> This created the possibility to *directly* assess the energetic stability of metal atoms within these metal nanoparticles and thus the strength of metal–oxide bonding. Furthermore, we have shown that the metal/oxide adhesion energy can be determined from the integral heat of metal adsorption on the oxide.<sup>5,16–22</sup> Thus, one can now hope to correlate the strength of metal–oxide bonding with the structural, electronic, chemisorption, and catalytic properties of oxide-supported metal particles, their dispersion, and their resistance to long-term sintering. Here, we analyze our recent measurements of metal adsorption energies and adhesion energies on the MgO(100) surface,<sup>16–22</sup> and correlate them with elemental properties of the metal (e.g. the position of the metal in the periodic table, the heat of sublimation or heat of oxide formation of the metal, plasmon energy, etc.). These correlations give new insight into the mechanisms of metal–oxide bonding. We also relate the measured energies to

the resulting metal film morphology (size and number density of particles) and the metal atom's sticking probability ( $S$ ). These correlations reveal trends of general interest to any thin film growth system.

There have been some previous attempts to correlate elemental properties of molten metals with their adhesion energies on alumina, silica, and ZrO<sub>2</sub>, measured by contact angle and related methods. Chatain et al. showed that the adhesion energies increase with the enthalpy of formation of the oxide (per mole of oxygen)<sup>23–26</sup> (with a second term which accounts for the estimated strength of metal–metal bonds at the interface), when divided by the area per metal atom, to convert energies from “per mole” to “per unit area”. This correlation suggests that adhesion energies are determined by the strength of *local* chemical bonds formed at the interface, both metal–oxygen and metal–metal. The adhesion energy of metals on oxides was also observed to increase as the plasmon energy of the metal increases<sup>27</sup> and increase with decreasing oxide band gap<sup>27</sup> or high-frequency dielectric constant.<sup>28</sup> Didier et al. showed that an approximate dielectric continuum model reproduces these trends and even *overestimates* adhesion energies while completely neglecting local chemical bonds.<sup>27</sup> This suggests a completely different picture where the adhesion energy of a metal to an oxide is dominated by the *long-range* dielectric continuum response of the two materials.<sup>27,29</sup> It was thus unclear which of these two physical pictures is most appropriate. Our results below show no correlation of the low-coverage adsorption energies of metals on MgO(100) with their plasmon energies nor with the enthalpies of formation of their oxides but do show a strong correlation with the enthalpies of sublimation of the bulk metals, suggesting that local metal–Mg bonding, rather than metal–oxygen bonding, dominates the interaction. The adhesion energies for 3D metal films correlate with the sum of magnitudes of the metal's sublimation energy plus the enthalpies of formation of its oxide, suggesting that both local metal–Mg and metal–oxygen bonds contribute to the interfacial bonding.

There have been a number of state-of-the-art quantum mechanical calculations of metal adsorption and adhesion energies on oxide surfaces,<sup>30–46</sup> many focusing on MgO(100). Since serious approximations must still be made in these

- (8) Persaud, R.; Madey, T. E. In *The Chemical Physics of Solid Surfaces and Heterogeneous Catalysis*; King, D. A., D. P. Woodruff, Eds.; Elsevier: Amsterdam, 1997; Vol. 8.
- (9) Rainer, D. R.; Goodman, D. W. *J. Mol. Catal. A* **1998**, *131*, 259.
- (10) Diebold, U.; Pan, J.-M.; Madey, T. E. *Surf. Sci.* **1995**, *331–333*, 845.
- (11) Lad, R. *J. Surf. Rev. and Lett.* **1995**, *2*, 109.
- (12) Adamson, A. W. *Physical Chemistry of Surfaces*, 5th ed.; John Wiley and Sons: New York, 1990.
- (13) Wu, M.-C.; Goodman, D. W. *J. Phys. Chem.* **1994**, *98*, 9874.
- (14) Wu, M.-C.; Oh, W. S.; Goodman, D. W. *Surf. Sci.* **1995**, *330*, 61.
- (15) Campen, D. G. V.; Hrbek, J. *J. Phys. Chem.* **1995**, *99*, 16389.
- (16) Stuckless, J. T.; Starr, D. E.; Bald, D. J.; Campbell, C. T. *J. Chem. Phys.* **1997**, *107*, 5547.
- (17) Stuckless, J. T.; Frei, N. A.; Campbell, C. T. *Rev. Sci. Instrum.* **1998**, *69*, 2427.
- (18) Ranney, J. T.; Starr, D. E.; Musgrove, J. E.; Bald, D. J.; Campbell, C. T. *Faraday Discuss.* **1999**, *114*, 195.
- (19) Larsen, J. H.; Ranney, J. T.; Starr, D. E.; Musgrove, J. E.; Campbell, C. T. *Phys. Rev.* **2001**, *B 63*, 195410.
- (20) Larsen, J. H.; Starr, D. E.; Campbell, C. T. *J. Chem. Thermodyn.* **2001**, *33*, 333.
- (21) Starr, D. E.; Bald, D. J.; Musgrove, J.; Ranney, J.; Campbell, C. T. *J. Chem. Phys.* **2001**, *114*, 3752.
- (22) Starr, D. E.; Campbell, C. T. *J. Phys. Chem.* **2001**, *B105*, 3776.

- (23) Chatain, D.; Rivollet, I.; Eustathopoulos, N. *J. Chim. Phys.* **1986**, *83*, 561.
- (24) Chatain, D.; Rivollet, I.; Eustathopoulos, N. *J. Chim. Phys.* **1987**, *84*, 201.
- (25) Chatain, D.; Coudurier, L.; Eustathopoulos, N. *Rev. Phys. Appl.* **1988**, *23*, 1055.
- (26) Sangiorgi, R.; Muolo, M. L.; Chatain, D.; Eustathopoulos, N. *J. Am. Ceram. Soc.* **1988**, *71*, 742.
- (27) Didier, F.; Jupille, J. *Surf. Sci.* **1994**, *314*, 378.
- (28) Stoneham, A. M.; *Appl. Surf. Sci.* (**1982–1983**), *14*, 249.
- (29) Tasker, P. W.; Stoneham, A. M. *J. Chim. Phys.* **1987**, *84*, 149.
- (30) Musolino, V.; Selloni, A.; Car, R. *J. Chem. Phys.* **1998**, *108*, 5044.
- (31) Musolino, V.; Selloni, A.; Car, R. *Surf. Sci.* **1998**, *402–404*, 413.
- (32) Heifets, E.; Zhukovskii, Y. F.; Kotomin, E. A.; Causa, M. *Chem. Phys. Lett.* **1998**, *283*, 395.
- (33) Neyman, K. M.; Vent, S.; Pacchioni, G.; Rosch, N. *Nuovo Cimento* **1997**, *19*, 1743.
- (34) Neyman, K.; Vent, S.; Rösch, N.; Pacchioni, G. *Top. Catal.* **1999**, *9*, 153.
- (35) Neyman, K. M.; Rösch, N.; Pacchioni, G. *Appl., Catal. A* **2000**, *191*, 3.
- (36) Pacchioni, G.; Rösch, N. *Surf. Sci.* **1994**, *306*, 169–178.
- (37) Pacchioni, G.; Rosch, N. *J. Chem. Phys.* **1996**, *104*, 7329.
- (38) Pacchioni, G.; Rösch, N. *J. Chem. Phys.* **1996**, *104*, 7329.
- (39) Pacchioni, G.; Lopez, N.; Illas, F. *Faraday Discuss.* **1999**, *114*, 209.
- (40) Yudanov, I.; Pacchioni, G.; Neyman, K.; Rosch, N. *J. Phys. Chem. B* **1997**, *101*, 2786.
- (41) Yudanov, I.; Vent, S.; Neyman, K.; Pacchioni, G.; Rosch, N. *Chem. Phys. Lett.* **1997**, *275*, 245.
- (42) Peri, S. S.; Lund, C. R. F. *J. Catal.* **1995**, *152*, 410.
- (43) Lopez, N. *J. Chem. Phys.* **2001**, *114*, 2355.
- (44) Giordano, L.; Pacchioni, G.; Bredow, T.; Sanz, J. F. *Surf. Sci.* **2001**, *471*, 21.

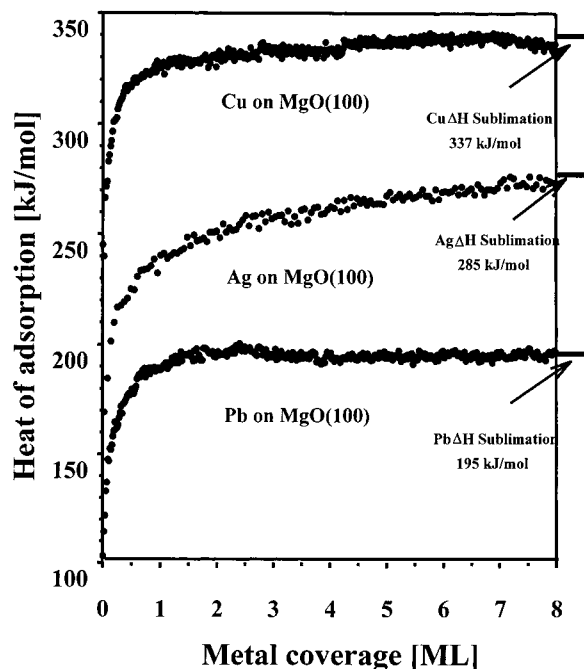


**Figure 1.** Standard enthalpies of adsorption of Cu, Ag, and Pb on MgO(100) at 300 K, from refs 18, 19, and 21. Also shown are the literature values for the bulk sublimation enthalpies at 300 K, from ref 76.

calculations, the experimental values can serve as benchmarks to help theorists decide which approximations are acceptable. The bonding mechanisms revealed by the trends mentioned above should also be helpful in this respect.

## II. Experimental Section

The calorimetry methods have been described in detail in the original papers from which these data are extracted.<sup>18,19,21</sup> The MgO(100) surface was grown in the form of a thin film on a 1- $\mu\text{m}$  thick Mo(100) crystal by dosing high purity (99.9+%) Mg in O<sub>2</sub> gas with subsequent annealing to  $\sim 750$  K as pioneered by Wu et al.<sup>47,48</sup> and described in more detail in refs 18–21. The MgO(100) film was  $\sim 4$ -nm thick as estimated from AES analysis. The (1  $\times$  1) square symmetry pattern observed with LEED was of similar quality as in refs 47,48. The LEED spot widths indicate a high step density, with terrace widths of only  $\sim 10$  nm. The MgO(100) surface was kept at room temperature (300 K) for all experiments.

## III. Calorimetric Measurements of Metal Adsorption and Adhesion Energies on MgO(100)

Figure 1 shows the heats of adsorption of Cu, Ag, and Pb on MgO(100) as a function of coverage.<sup>16–22</sup> Here, a pulsed beam of metal vapor (>99% free atoms) impinges on the MgO(100) surface, and the transient temperature rise associated with the adsorption of each  $\sim 0.02$  monolayer pulse of metal is recorded with a pyroelectric heat detector. Precision of  $\pm 1$ –2% (4–10 kJ/mol pulse-to-pulse standard deviation) and absolute accuracy

of  $\pm 1$ –2% are observed. As shown for all three metals, the measured heat of adsorption starts out quite low and then increases rapidly with metal coverage until it reaches a value within 1% of the sublimation enthalpy of the bulk metal solid. The very low initial heat of adsorption is a combination of the following two effects: (1) the metal particles are very small so that the average metal atom is stabilized by far fewer nearest neighbor bonds than when present in bulk metal form, and (2) the downward bonding of the metal to the MgO is weaker than the downward bonding between, for example, the metal atoms in the topmost atomic layer of a bulk metal (100) surface and the metal atoms in its second layer. As the particle size and thickness increase with coverage, these effects become less important in their influence on the adsorption energy of subsequent metal atoms so that it eventually reaches the large-particle limit.

A simple thermodynamic cycle we derived elsewhere<sup>5,16</sup> shows the mathematical relationship between adsorption and adhesion energies:

$$AE_{\text{adh}} = -\sum_n \Delta H_{\text{adsorption}} - n\Delta H_{\text{sublimation}} + A(1+f)\gamma_{\text{v/m}} \quad (1)$$

Here,  $-\sum_n \Delta H_{\text{adsorption}}$  is the integral of the adsorption enthalpy versus coverage over the first  $n$  metal atoms (a thick multilayer coverage),  $A$  is the area they cover,  $f$  is the surface roughness factor for this metal film,  $\gamma_{\text{v/m}}$  is the surface energy of the clean, bulk solid metal,  $E_{\text{adh}}$  is its adhesion energy to the substrate, and  $\Delta H_{\text{sublimation}}$  is the bulk sublimation enthalpy of the metal. We have used this relationship to determine the adhesion energies of the metals from the integral adsorption enthalpy measured between 0 and  $\sim 10$  ML and presented in Figure 1. The resulting adhesion energies are summarized in Table 1.

We estimate the strength of metal–MgO bonds from the calorimetry results assuming pairwise bond additivity. While this model is inaccurate in details, it has been used with great success in understanding qualitative aspects of chemical bonding and organic reactions;<sup>49</sup> therefore we use it here as a first-order approximation. Within this model, the energy of a metal–metal bond,  $E(\text{M}–\text{M})$ , is just  $1/6$  of the metal's bulk cohesive energy (i.e., its sublimation energy) for FCC and HCP metals, since atoms in these structures have 12 nearest neighbors and all the bond energies are shared by two atoms. We define the metal–MgO bond energy,  $E(\text{M}–\text{MgO})$ , as the average total bond energy between one metal (M) atom in the first layer and the MgO(100) surface. (Thus, it is the sum of *all* pairwise bonds between the average interfacial metal atom and all Mg and O atoms below.) This bond energy can be estimated from the adsorption energy measured during the first pulse of metal–vapor deposition, provided that pulse produces small metal islands of known size and shape. In the pairwise bond additivity model, this adsorption energy is just the sum of bond energies for all the M–M nearest neighbor bonds in the island plus the number of M–MgO bonds at the interface, divided by the total number of atoms in the island. Since the approximate island size and shape (2D platelets close to one atom thick) are known at very low coverages from AES for Ag and Pb adsorption on MgO(100),<sup>19,21,50</sup> we were able to estimate the Ag–MgO and Pb–

(45) Giordano, L.; Pacchioni, G.; Ferrari, A. M.; Illas, F.; Rosch, N. *Surf. Sci.* **2001**, *473*, 213.

(46) Giordano, L.; Goniakowski, J.; Pacchioni, G. *Phys. Rev. B* **2001**, *6407*, 075417.

(47) Wu, M.-C.; Corneille, J. S.; Estrada, C. A.; He, J.-W.; Goodman, D. W. *Chem. Phys. Lett.* **1991**, *182*, 472.

(48) Wu, M.-C.; Corneille, J. S.; He, J.-W.; Estrada, C. A.; Goodman, D. W. *J. Vac. Sci. Technol., A* **1992**, *10*, 1467.

(49) Benson, S. W. *Thermochemical Kinetics*; John Wiley and Sons: New York, 1976.

(50) Didier, F.; Jupille, J. *Surf. Sci.* **1994**, *307*–309, 587.

**Table 1.** Summary of Metal–MgO(100) Bonding Energetics and Some Bulk Properties of the Metals on Their Oxides; Calorimetry Data and Bulk Metal Surface Energies for Cu, Ag, and Pb from refs 18, 19, and 21; Adhesion Energy for Pd from refs 58,59; Bulk Enthalpies from ref 76; Bulk Plasmon Energies from refs 27 and 77; Adhesion Energies of Molten Metal Drops on Alumina and Silica from ref 5

metal	calorimetry 2D Platelets		calorimetr 3D Particles		bulk properties of the metals (literature values)					molten droplet's $E_{\text{adhesion}}$ ( $\mu\text{J}/\text{cm}^2$ )	
	initial $\Delta H_{\text{ads}}$ (kJ/mol M)	2D M–MgO bond energy (kJ/mol M)	$E_{\text{adhesion}}$ ( $\mu\text{J}/\text{cm}^2$ )	3D M–MgO bond energy (kJ/mol M)	$-\Delta H_{\text{f,ox}}$ (kJ/molM)	metal's surface energy ( $\mu\text{J}/\text{cm}^2$ )	$\Delta H_{\text{sublim}}$ (kJ/molM)	$(\Delta H_{\text{sublim}} - \Delta H_{\text{f,ox}})$ (kJ/molM)	plasmon energy (eV)	on $\text{Al}_2\text{O}_3$	on $\text{SiO}_2$
Pb	103 ± 2	32 ± 2	77 ± 20	49 ± 15	277	59	195	472	13.5	17 ± 4	21
Ag	176 ± 3	110 ± 3	30 ± 30	15 ± 15	16	122	285	301	3.8	32	17
Cu	240 ± 3	198 ± 4	192 ± 60	78 ± 23	157	176	337	494	8.1	49	47
Pd			(91)	(42)	85	164	377	462	7.7	74	

MgO bond energies in this way from the heat measured in the first pulse, as described in detail elsewhere.<sup>19,21</sup> Since Cu grows as 2D islands up to at least 0.3 ML,<sup>18</sup> we have assumed that by this coverage the islands are so large that edge effects are negligible. Thus, the differential heat of adsorption at this coverage is just  $E(\text{Cu–MgO}) + \{E(\text{Cu–Cu}) \times N/2\}$ , where  $N$  is the number of nearest neighbors Cu atoms for a Cu atom in these large 2D islands. Since LEED shows that the Cu grows as Cu(100) epitaxially on the MgO(100),<sup>51</sup> we assume these 2D islands have Cu(100)-like structure with each atom then having four nearest neighbors ( $N = 4$ ). This gives  $E(\text{Cu–MgO}) = 198$  kJ/mol from the measured heat of adsorption at this coverage (310 kJ/mol). This is somewhat of an underestimate since island edge effects would actually reduce  $N$ . (This value is 34% larger than we previously estimated, assuming instead Cu(111)-like structure within these 2D islands,<sup>18</sup> which gave  $E(\text{Cu–MgO}) = 141$  kJ/mol but is probably less accurate. The correlations discussed below are equally valid with the old value.) Note that the initial heat of adsorption (for the first 0.025 ML) is 240 kJ/mol, which certainly sets an upper limit to  $E(\text{Cu–MgO})$  since this heat no doubt includes contributions from Cu–Cu bonding in tiny 2D islands. This is consistent with the value of 198 kJ/mol estimated above. These values for M–MgO bond energies at the interface of 2D metal islands are listed in Table 1.

The adhesion energies have been converted into metal–MgO bond energies by simply dividing by the number of metal atoms per unit area at the interface, assuming Cu(100), Ag(100), and Pb(111) packing (see Figure 2). (The 111 epitaxy for Pb is expected due to the large lattice mismatch.<sup>5</sup>) These values for M–MgO bond energies at the interface between  $>8$  layer-thick metal films (or large particles in the case of Pb) are listed also in Table 1.

Notice that these Cu–MgO bond energies for multilayer films are much smaller than those listed for the interface of 2D metal platelets. This is partially because pairwise bond additivity fails. The strength of bonds between a Cu atom and its neighbors is clearly stronger when the Cu atom is in 2D islands, which we attribute partially to the fact that it has fewer nearest neighbors there than at the interface of a multilayer film. It is very common that the bond energy between an atom and its neighbors gets smaller when the atom gets more neighbors, as we see here. For example, the bond strength between two carbon atoms decreases from  $\sim 800$  to 378 kJ/mol as the number of H atoms bonded to each of those two C atoms increases from one to three.<sup>52,53</sup> Such three-body effects are well-known to be strong

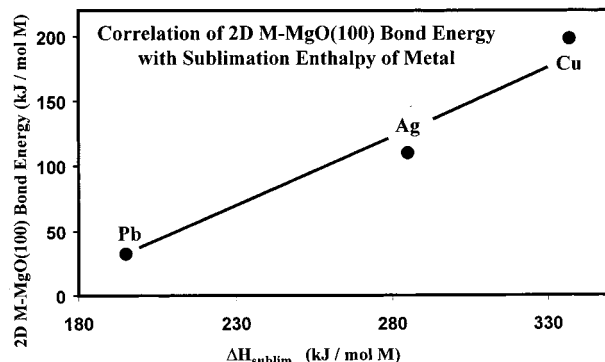


**Figure 2.** The 2D M–MgO bond energy (i.e., the total attraction per metal atom in 2D metal islands to the MgO(100) surface, estimated from the measured heat of adsorption using a pairwise bond additivity model to remove contributions from M–M bonding) plotted versus the heat of sublimation of the metal. We propose that the heat of sublimation reflects the strength with which that metal can covalently bind to other metal atoms, in this case the strength of M–Mg covalent bonds, which thus appear to dominate the interfacial binding.

in metal–metal bonding. Density functional calculations show that the average M–M bond energy decreases strongly as the average coordination number of the metal atom increases.<sup>54</sup> Note that this also means that the M–M bonds within the 2D platelet will also be stronger than in the large 3D particles. Of course, within this bond-additivity approximation, we have thrown all of that extra stabilization falsely into the single variable parameter in the model,  $E(\text{M–MgO})$ . Another reason that the 2D platelets bind so much more strongly to the MgO than to the 3D films is that they can relax their lattice mismatch with the MgO much more easily to optimize stability, whereas the thick 3D films are forced to achieve the bulk metal structure eventually. Any lattice strain involved lowers  $E(\text{M–MgO})$ , since the bond additivity approximation bunches all such effects into this one parameter when we hold  $E(\text{M–M})$  constant at its bulk value. Finally, the larger  $E(\text{M–MgO})$  for 2D islands is related to the fact that they generally nucleate at defects which bind metals more strongly.<sup>1,4,5,55,56</sup> For example, Giordano et al. found from DFT calculations that an isolated Pd adatom binds to an oxygen vacancy with an energy 2.6 times that at its favorite site on defect-free MgO(100),<sup>46</sup> and that this vacancy triples the binding energy of  $\text{Ni}_4$  and  $\text{Ni}_8$  clusters to MgO(100).<sup>57</sup> This effect of defects is probably especially important for the very tiny 2D particles used in getting the metal–MgO bond energies

(53) McMillen, D. F.; Golden, D. M. *Annu. Rev. Phys. Chem.* **1982**, *33*, 493–532.

(54) Methfessel, M.; Hennig, D.; Scheffler, M. *Appl. Phys.* **1992**, *A55*, 442.

(55) Venables, J. A.; Harding, J. H. *J. Crystal Growth* **2000**, *211*, 27.

(56) Henry, C. R.; Chapon, C.; Duriez, C.; Giorgio, S. *Surf. Sci.* **1991**, *253*, 177.

(57) Giordano, L.; Pacchioni, G.; Illas, F.; Rosch, N. *Surf. Sci.* **2002**, *499*, 73.

(51) He, J.-W.; Möller, P. J. *Surf. Sci.* **1986**, *178*, 934.

(52) Hendrickson, J. B.; Cram, D. J.; Hammond, G. S. *Organic Chemistry*; McGraw-Hill: New York, 1970.

for Ag and Pb in Table 1. (The Ag and Pb particles contained, on average,  $\sim 14$  and 20 atoms, respectively.)

Graoui et al.<sup>58,59</sup> measured the equilibrium shapes of solid Pd nanoparticles on MgO(100) by electron microscopy, and from this estimated the “apparent adhesion energy” using the Wulff–Kaisheff theorem. They found it to increase from 91 to  $> 164 \mu\text{J}/\text{cm}^2$  with decreasing Pd particle size in the 15–3 nm range. This must be at least partially for the same reasons as outlined above. They found that the lattice of Pd particles smaller than 5 nm dilated to match the MgO lattice parameter. The adhesion energy they found for their largest Pd particles and the corresponding Pd–MgO bond energy we estimate from it (assuming Pd(100) packing density at the interface) are entered in Table 1.

#### IV. Correlations of Energetics with Bulk Metal Properties

As can be seen in Table 1, the initial adsorption energy and the M–MgO bond energy for 2D metal islands increase in the series  $\text{Pb} < \text{Ag} < \text{Cu}$ . Since the heat of adsorption at any coverage increases in this same sequence, it is clear that this trend in bond energies is true despite the inaccuracies of pairwise bond additivity and our estimates of island sizes used to get the bond energies. This is especially clear when one realizes that island sizes increase in the opposite direction ( $\text{Cu} < \text{Ag} < \text{Pb}$ , see below), so that the number of metal–metal bonds contributing to the average heat increases as  $\text{Cu} < \text{Ag} < \text{Pb}$ . The adhesion energies on MgO(100) in Table 1 follow the series  $\text{Ag} < \text{Pb} < \text{Pd} < \text{Cu}$ . Adhesion energies of molten metals measured by contact angle methods on alumina and silica,<sup>5</sup> are also listed in Table 1. (These are actually works of adhesion, and we have equated them to adhesion energies by neglecting the entropic contribution.) They increase as  $\text{Pb} < \text{Ag} < \text{Cu} < \text{Pd}$  on alumina and as  $\text{Ag} < \text{Pb} < \text{Cu}$  on silica. The values of the adhesion energies for a given metal are smaller on these oxides than our values on MgO(100), which is possibly because the values for MgO are for solid rather than liquid metal and because the other oxide surfaces were not in UHV and therefore not as clean.

For comparison to the calorimetric results on MgO(100), Table 1 also lists the enthalpy of formation of the most stable bulk oxide of each metal (per mole of metal),  $\Delta H_{\text{f,ox}}$ , and each metal's bulk sublimation enthalpy,  $\Delta H_{\text{sublim}}$ , which equals in magnitude its bulk cohesive energy. Earlier studies of adhesion energies<sup>60</sup> suggested a correlation between adhesion energies and the heats of formation of the oxide of the metal. The heats of adsorption, adhesion energies, and M–MgO bond energies do *not* correlate well with the enthalpy of formation of the oxide. This suggests that the interfacial bonding is not dominated by the strength of local chemical bonds between the metal atoms and the oxygen atoms of the substrate. Note that there is a good correlation between the heats of adsorption and M–MgO bond energies for 2D islands of these four metals and their bulk cohesive energies (or sublimation enthalpies). This suggests that whatever property of a metal determines the strength with which it binds to other metal atoms in its bulk also determines its ability to bind to the MgO(100) surface (as well as  $\text{Al}_2\text{O}_3$  and silica).

That property is probably the strength of its local covalent (metallic) bonding to other metal atoms, assuming that a metal's bulk cohesive energy reflects the strength of its local covalent bonding to other metal atoms, whether the same element or another metal element. In agreement with this picture are quantum calculations of metal/alumina interfaces by Jarvis and Carter, which suggested that metal–metal bonds are very important in determining the strength of interfacial attraction.<sup>61</sup> This is countered by X-ray diffraction measurements<sup>62,63</sup> and quantum calculations<sup>32,40,64–69</sup> which consistently show that Ag, Cu, and Pd adatoms, when present as close-packed  $p(1 \times 1)$  monolayers or as more isolated adatoms, prefer to sit on the oxygen sites of a perfect MgO(100) lattice, which certainly suggests that these metals bond mainly to the oxygen atoms of the MgO lattice, (although the distance to the four nearest Mg ions at this site may allow a great deal of M–Mg bonding). This seems, however, inconsistent with the lack of correlation of the M–MgO bond energies with the heat of formation of the metal's oxide, which should reflect the strength of the metal–oxygen bonds involved.

One possible resolution of this apparent contradiction would be to recognize that MgO(100) lattice defects, estimated to be present at the  $\sim 4\%$  level from our LEED spot widths, may be playing a major role here. When a metal adsorbs at step edges and oxygen vacancies, its bonding to under-coordinated Mg atoms is probably more important than bonding to oxygens. The observation that metal clusters nucleate at defects on MgO(100)<sup>4,55,56</sup> shows that such binding to defects is much stronger, consistent with recent quantum calculations.<sup>46,70</sup> For example, calculations predict that Pd bonds 2.6 times as strongly to an oxygen vacancy than to defect-free MgO(100).<sup>46</sup> This factor should be even larger at step edges. Such large increases could mean that metal–Mg bonding at defects dominates the bond energy of a tiny cluster to the MgO, even when most of its atoms are not at defects. Metal atoms tied to defects may also direct neighboring metal atoms into sites other than the oxygen sites they prefer when isolated on a terrace, due to the strong driving force to optimize metal–metal bonding.

It should be noted that the increase in the 2D M–MgO bond energy with sublimation energy shown in Table 1 is somewhat exaggerated by the use of the bond additivity approximation above. The metal–metal bonds within the 2D clusters are actually stronger than the metal–metal bonds in bulk metal, as noted above. The amount that they are stronger for a given cluster size is probably roughly proportional to the bulk sublimation energy. Since this was not taken into account, the 2D M–MgO BEs in Table 1 are overestimated by an amount roughly proportional to the bulk sublimation energy. We estimated within various models that this is not the dominant effect, however, so that the increase of M–MgO bond energy with sublimation energy is still quite valid. Confirming this, the initial heat of adsorption increases also with the sublimation

(58) Graoui, H.; Giorgio, S.; Henry, C. R. *Surf. Sci.* **1998**, *417*, 350.

(59) Graoui, H.; Giorgio, S.; Henry, C. R. *Philos. Mag. B* **2001**, *81*, 1649–58.

(60) Peden, C. H. F.; Kidd, K. B.; Shinn, N. D. *J. Vac. Sci. Technol.* **1991**, *A9*, 1518.

(61) Jarvis, E. A. A.; Christensen, A.; Carter, E. A. *Surf. Sci.* **2001**, *487*, 55.

(62) Flank, A. M.; Delaunay, R.; Lagarde, P.; Pompa, M.; Jupille, J. *Phys. Rev. B* **1996**, *53*, R1737.

(63) Renaud, G.; Barbier, A.; Robach, O. *Phys. Rev. B* **1999**, *60*, 5872.

(64) Li, C.; Wu, R.; Freeman, A. J.; Fu, C. L. *Phys. Rev. B* **1993**, *48*, 8317.

(65) Lopez, N.; Illas, F.; Rösch, N.; Pacchioni, G. *J. Chem. Phys.* **1999**, *110*, 4873.

(66) Lopez, N.; Illas, F. *J. Phys. Chem. B* **1998**, *102*, 1430.

(67) Goniakowski, J. *Phys. Rev. B* **1999**, *59*, 11047.

(68) Goniakowski, J. *Phys. Rev. B* **1998**, *57*, 1935.

(69) Goniakowski, J. *Phys. Rev. B* **1998**, *58*, 1189.

(70) Bogicevic, A.; Jennison, D. R. *Surf. Sci. Lett.* **1999**, *437*, L741.

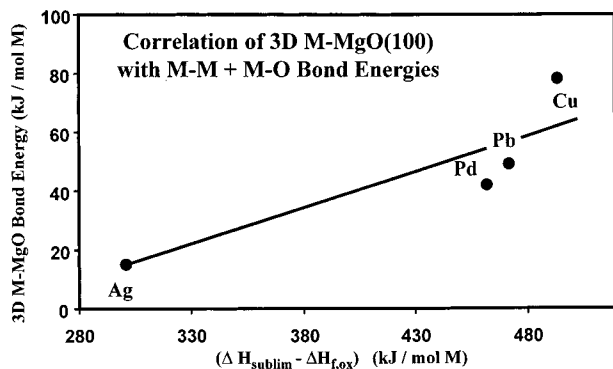


**Figure 3.** The 3D M–MgO bond energy (i.e., the total attraction per metal interface atom in thick, 3D metal films to the MgO(100) surface, estimated from the measured adhesion energy using a pairwise bond additivity model to remove contributions from M–M bonding) plotted versus the difference between the heat of sublimation of the metal and the heat of formation of the metal's most stable oxide, per mole of metal. This difference should reflect the combined strength of M–Mg and M–O bonds. Adhesion energy for Pd from refs 58, and 59.

energy, even though the size of metal clusters created in this first pulse increases in the opposite direction ( $\text{Cu} < \text{Ag} < \text{Pb}$ ).

The metal's ability to respond to longer-range electrostatic forces such as the instantaneous dipoles of a nearby lattice or the Madelung field of an oxide should increase with its bulk plasmon energy, according to Didier.<sup>27</sup> As shown in Table 1, the adsorption and adhesion energies of the metals do *not* correlate with their plasmon energies, nor do their extracted M–MgO bond energies.

The adhesion energies and corresponding M–MgO bond energies for 3D films (or thick particles) show a crude correlation with the sublimation enthalpy of the four metals in Table 1 (see Figure 3). However, the correlation improves markedly if we make comparisons instead to the sum of the sublimation enthalpy and the magnitude of  $\Delta H_{f,ox}$  of the metal's oxide, also shown in Table 1. The M–MgO bond energies increase uniformly with this sum,  $\Delta H_{sublim} + (-\Delta H_{f,ox})$ . This suggests that there is an equally important contribution to the interfacial binding of 3D metal films to MgO(100) due to local metal–oxygen bonds at the interface, as well as the local, covalent metal–Mg bonding. The metal–Mg bonds dominate for 2D islands, possibly because of the greater importance of defects for the 2D measurements than for the 3D measurements, where the metal film covers a greater fraction of the surface. It is also possible that M–Mg bonds increase in strength much more than M–O bonds when in the lower coordination environment of 2D islands (compared to 3D films). The important contributions from both metal–Mg and metal–oxygen bonding in the 3D case, suggested by this correlation, is consistent with both the dominance of covalent metal–Mg bonding at defects mentioned above for the 2D case (but reduced in importance for the 3D case) and the dominance of metal–oxygen bonding at perfect terrace sites suggested by the preference of metal atoms for oxygen sites on perfect MgO(100) terraces.<sup>32,40,64–69</sup> Calculations of Pd/MgO(100) by Giordano et al.<sup>46</sup> also predicted this decreasing role of defects with increasing metal film thickness.

The increase in M–MgO bond energies with the function  $[\Delta H_{sublim} + (-\Delta H_{f,ox})]$  is quite similar to a correlation observed by Chatain et al.<sup>23–26,71,72</sup> for the adhesion energies of molten metals (M) on  $\text{Al}_2\text{O}_3$ ,  $\text{SiO}_2$ , and  $\text{ZrO}_2$ , who showed that adhesion

**Table 2.** Comparison of the Initial Heats of Adsorption of Metals on MgO(100) with Their Initial Sticking Probabilities,  $S(0)$ , Measured Mass-Spectrometrically, and Saturation Island Densities,  $N$ , Estimated from AES Intensities versus Coverage Using a Hemispherical Cap Model (Data from refs 18,19,21)

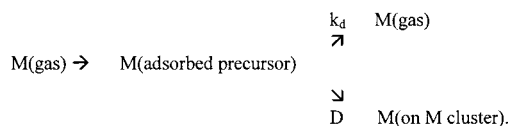
metal	initial $\Delta H_{ads}$ (kJ/mol)	$S(0)$	island density ( $\text{cm}^{-2}$ )
Pb	$103 \pm 2$	0.70	$8 \times 10^{11}$
Ag	$176 \pm 3$	0.943	$2.5 \times 10^{12}$
Cu	$240 \pm 3$	0.997	$>3 \times 10^{12}$

energies increase with the function:  $[\Delta H_{f,alloy} + \Delta H_{f,ox}]/V_M^{2/3}$ , where  $\Delta H_{f,alloy}$  is the enthalpy of formation of the M–Me alloy (with Me = Al, Si, or Zr) per mole M (at infinite dilution) and  $V_M$  is the molar volume of the molten metal. The factor  $V_M^{-2/3}$  simply converts energies per mole M to energies per unit area, for direct comparison to adhesion energies per unit area. This conversion is essentially the reverse of that used in Table 1 to convert adhesion energies to M–MgO bond energies per mole M. This correlation of adhesion energies with  $[\Delta H_{f,alloy} + \Delta H_{f,ox}]/V_M^{2/3}$  is essentially identical to our correlation of the M–MgO bond energies with  $\Delta H_{sublim} - \Delta H_{f,ox}$ , if we assume that  $\Delta H_{f,alloy}$  for these M–Mg alloys varies proportional to  $-\Delta H_{sublim}$ . Unfortunately, Chatain et al. did not explain how they found their values for  $\Delta H_{f,alloy}$ . Their correlation, however, gives further support to our hypothesis that local metal–Me covalent bonding is very important in determining the strength of the metal/oxide interfacial bonding. By this, we do not mean to imply that the M–Mg bonds are entirely covalent but rather that covalent bonding (i.e., the sharing of electrons) is a very important contributor to the total bond strength. Indeed, it appears to dominate the bonding of the 2D islands to the MgO.

Just as seen here for the M–MgO bond energies for 2D islands, and the adhesion energies on alumina,<sup>25</sup> the adhesion energies measured by contact angle methods for molten metal droplets on titanium carbide increase in the series  $\text{Pb} < \text{Ag} < \text{Cu}$ .<sup>73</sup> This suggests that there may be a more general validity to this increase in the metal/oxide (or metal/carbide) attraction with the metal's sublimation energy, and its implication with respect to the dominant interfacial bonding mechanism (i.e., local covalent metal–Me bonding, possibly with a strong contribution from defects).

## V. Correlations of Energetics with Sticking Probabilities and Film Morphology

Both the initial sticking probability,  $S(0)$ , and the island density,  $N$ , measured for these metals on MgO(100) at 300 K increase with the initial adsorption energy or M–MgO bond energy of the metal, as shown in Table 2. Following Zhou et al.,<sup>74</sup> we propose the following mechanism for metal sticking to MgO(100):



(71) Rivollet, I.; Chatain, D.; Eustathopoulos, N. *Acta Metall.* **1987**, *35*, 835.

(72) Hicter, P.; Chatain, D.; Pasturel, A.; Eustathopoulos, N. *J. Chim. Phys.* **1988**, *85*.

(73) Jianguo, L. *Rare Met.* **1992**, *11*, 177.

(74) Zhou, J. B.; Lu, H. C.; Gustafsson, T.; Garfunkel, E. *Surf. Sci.* **1993**, *293*, L887.

Thus, it is assumed that all incident metal atoms get trapped temporarily in a mobile precursor state, from which it can either desorb or attach to a cluster. The measured sticking probability ( $S$ ) refers to the fraction of adatoms that follow the latter branch. Here  $k_d$  refers to the desorption rate constant for the isolated metal adatom, which is related to its adsorption energy,  $E_{ad,monomer}$ , by  $k_d = \nu \exp[-E_{ad,monomer}/(RT)]$ , with  $\nu$  being  $\sim 10^{13} \text{ s}^{-1}$ . Also,  $D$  refers to the diffusive jump frequency for this monomer, which is crudely approximated by  $D = \nu \exp[-\chi E_{ad,monomer}/(RT)]$ , where  $\chi$  is some factor typically between 0.1 and 0.4.<sup>55,75</sup> Because  $\chi$  is a small fraction of 1, it is clear that a change in  $E_{ad,monomer}$  will manifest itself much more strongly in  $k_d$  than  $D$ . Thus, increasing  $E_{ad,monomer}$  will decrease the ratio  $k_d/D$  and thus decrease the desorption probability and increase the sticking probability, if the density of clusters is approximately the same. Since the initial heats of adsorption and M–MgO bond energies increase in the sequence Pb < Ag < Cu, we assume that  $E_{ad,monomer}$  follows the same trend, so that the sticking probability should increase as Pb < Ag < Cu, as observed. Because this effect is so strong, it overpowers the effect of the corresponding small increase in island density on the sticking probability. This effect, however, should also increase the sticking probability in the same direction: Pb < Ag < Cu. As the metal coverage increases, the islands eventually get so near together that desorption becomes unimportant.

(75) Venables, J. A. *Surf. Sci.* **1994**, 299/300, 798.

(76) *CRC Handbook of Chemistry and Physics*; Lide, D. R., Ed.; CRC Press: Boston, 1996.

(77) Lemonnier, J. C.; Priol, M.; Robin, S. *Phys. Rev.* **1973**, B8, 5452.

The increase in the saturation number density of islands ( $N$ ) in the sequence Pb < Ag < Cu is also consistent with this mechanism. In the limit of no desorption (i.e. unit initial sticking probability) for a critical nucleus size  $i = 1$ ,  $N$  varies as  $D^{-1/3}$  (for the similar metal vapor fluxes used here).<sup>75</sup> Since diffusion of metals on MgO(100) has a very low activation energy that scales roughly with  $E_{ad,monomer}$ <sup>55,75</sup>,  $D$  should increase in the sequence Cu < Ag < Pb. This gives a very weak increase of  $N$  with  $E_{ad,monomer}$ , in the same direction as our observations (Table 2). A much stronger dependence in this same direction is predicted for low sticking probability.<sup>75</sup>

Since the number density of islands is generally much smaller than the defect density on the surface, it is clear that the precursor states sample many defect sites before desorbing. Thus, both  $E_{ad,monomer}$  and  $D$  in the above mechanism refer to values which average over the metal adatom's transient residence times at both terrace and defect sites.

The saturation island density is expected to be the most important factor that determines the ultimate film morphology. The larger the island density, the smoother will be the resulting film.

**Acknowledgment.** We gratefully acknowledge Drs. Claude Henry and James Evans for very enlightening discussions, and the National Science Foundation for financial support during this work. One of the authors, D.E.S., also thanks the University of Washington Center for Nanotechnology for an NSF-IGERT graduate research fellowship.

JA020146T